Double polarization active Y junctions in the L band, based on Ti:$LiNbO_3$ lithium niobate waveguides: polarization and contrast performances

Samuel Heidmann,[1,*] Nadège Courjal,[2] and Guillermo Martin[1]

[1]*Université Joseph Fourier (UJF)-Grenoble 1/CNRS-Institut National des Sciences de l'Univers (INSU), Institut de Planétologie et d' Astrophysique de Grenoble (IPAG), UMR 5274, Grenoble, France*

[2]*Department of Optics P. M. Duffieux (LOPMD), Institut FEMTO-ST (UMR 6174), 16 Route de Gray, 25030-Besanon Cedex, France*

**Corresponding author: samuel.heidmann@obs.ujf-grenoble.fr*

Received April 18, 2012; revised June 11, 2012; accepted June 24, 2012; posted June 25, 2012 (Doc. ID 167056); published August 6, 2012

Double polarization electro-optic beam combiners based on a Ti:diffusion lithium niobate waveguide have been developed for mid-infrared applications. A monochromatic rejection ratio of up to 33 dB at $\lambda = 3.39$ μm was obtained, as well as wideband fringes showing low dispersion. In a first part, studying the fringe contrast as a function of waveguide width, we found a compromise among transmission, signal-to-noise ratio, and fringe contrast, depending on the single-mode behavior of the waveguides. We will show that both polarizations are guided, and at least 70% and 90% contrast is achieved, respectively, in TE and TM with a 400 nm wideband light centered at 3.39 μm. After choosing the optimal combiner and designing the electrodes, we studied the electro-optic response of the device, using a monochromatic source and scanning the fringe, by external as well as internal modulation, in order to determine the rejection ratio and the voltage needed to cover half a fringe (V_π) voltage for both TE and TM polarizations.

OCIS codes: 130.3730, 120.3180.

The mid-infrared (MIR) astronomical band L (3.4–4.1 m) is a key region to observe exoplanets and dust disks in the neighborhood of host stars by allowing the study of cool matter [1–3]. Furthermore, the star-to-planet brightness ratio makes the operation interesting beyond 3 μm, where this ratio reaches a minimum value around 10^{-4} for hot Jupiters and stellar dust. Stellar interferometry allows the observation of such objects at the milliarcsecond scale. Therefore, integrated optics (IO) active beam combiners are an interesting option regarding stability, modal filtering, real-time electrically controlled phase, and the ability to combine multiple apertures on a single chip [4,5]. Lithium niobate (LN)-based electro-optic modulators, commercially available for near-infrared applications, are known to achieve high bandwidth and deep rejection ratio [6,7]. As LN has good electro-optic efficiency, it is possible to electrically on-chip tune the optical path delay (OPD) between the two arms of the junction before combination. In this Letter, we present performances of IO beam combiners made by titanium diffusion in x-cut LN crystal. We show that this method is suitable to achieve both TE and TM polarization guidance, either for monochromatic or wideband applications.

Sample fabrication. The combiners consist of geometrically classical Y junctions, composed of straight segments with constant width where the Ti:diffusion parameters have been optimized to achieve single-mode guidance in the L band for both TE and TM polarization. The waveguides are built by depositing a 190-nm-thick titanium ribbon on the LN substrate and subsequently diffusing for 20 h. The width of the titanium ribbon goes from 12 to 26 μm by 2 μm steps. For the active device, aluminum electrodes have been deposited on the chip, at both sides of the first arm waveguide, and a silica buffer was used to ensure good adhesion.

Experimental setup. We developed two optical benches. First, in order to characterize dispersion, signal-to-noise ratio (SNR) and wideband contrast, a black body source was used. Second, for high contrast studies, a monochromatic 3.39 μm He–Ne CW laser was used. In both cases, light coming from the source is focused on a 20 μm diameter pinhole placed at the focal distance of an off-axis parabola (reflected focal length 25.4 mm). The collimated beam is separated by a thick ZnSe beam splitter in a Michelson setup. One arm is tunable in OPD, and the second one is slightly eccentric. These two beams are focused at the chip inputs, 250 μm separated, with a ZnSe lens ($f = 25.4$ mm). Therefore, as the collection and injection focal lengths are the same, the optical magnification is 1. The output of the chips are imaged with an IR camera. To measure spectral transmittance and differential dispersion between the two arms of the combiner, we externally scan the OPD with the motorized mounted mirror.

Monochromatic fringes. The mathematical expression of a monochromatic interferogram, assuming the source is nonresolved, is

$$I = I_1 + I_2 + 2 \cdot \sqrt{I_1 \cdot I_2} \cdot V \cdot \cos(\phi), \tag{1}$$

with I_1, I_2 as the photometry of arms 1 and 2; V as the visibility, and ϕ the phase difference at the junction. V can be expressed as the following product:

$$V = V_{\text{atm}} \cdot V_{\text{instr}} \cdot V_{\text{source}}, \tag{2}$$

with V_{atm} as visibility of atmosphere, V_{instr} the instrumental visibility, and V_{source} the visibility of the source.

V_{atm} can be assumed to be 1 since the waveguides are single mode at 3.39 μm. As the source is experimentally unresolved by our interferometer, we assume that $V_{\text{source}} = 1$. Thus, the parameter under study is the V_{instr}.

At first, the OPD is scanned externally. So ϕ can be expressed as [8]

$$\phi(x) = \phi_0 + 2\pi\sigma(x - x_0 + n_{\text{eff}}\Delta L) + \Delta\beta \cdot L_1, \quad (3)$$

with L_1 as the length of arm 1, ΔL the differential arm length, $\Delta\beta$ the propagation constant difference between arms, x the distance covered by the motorized mirror, x_0 the initial OPD between the two arms, ϕ_0 the initial phase difference between the two arms, n_{eff} the refractive index of the waveguide, and σ the wavenumber (λ^{-1}).

The differential arm length ΔL and the propagation constant difference $\beta_2 - \beta_1$ are responsible for contrast attenuation and fringe asymmetry. The normalized function for fringe contrast studies is [8]

$$I_{\text{corr}} = 1 + V_{\text{instr}} = 1 + \frac{I - I_1 - I_2}{2 \cdot \sqrt{I_1 \cdot I_2}}. \quad (4)$$

Passive junctions. For polychromatic measurements, we used a blackbody light source set up behind the pinhole and the motorized mirror to scan the OPD. The device has no electrodes and consists of Y junctions of increasing channel width, from 12 to 26 μm. As we aim at studying the guidance of the two polarizations, we place a polarizer and analyzer, respectively, at the input and output of the chip. The dispersion is theoretically related to the refractive index difference between the two arms of the combiners as a function of wavelength. If the two arms present the same dispersion, $\beta_1(\lambda) = \beta_2(\lambda)$ and the same length $\Delta L = 0$, there will be no differential effect and the junction will not be dispersive. This is what we experimentally observe. In Fig. 1, we observe a typical fringe packet obtained with the IO junction, in the TM and TE polarizations.

From Fig. 1 we observe very slight asymmetry, which leads us to conclude that the differential dispersion between the two arms is not significant. As the dispersion is negligible, the expected contrast in the combiner is then only limited to the modal filtering capabilities of the waveguide and the efficient destructive overlap of the optical beam at the recombination point (junction). We present in Fig. 2 a synthesis of the Y-junction performances for the two polarizations as a function of the width of the waveguides.

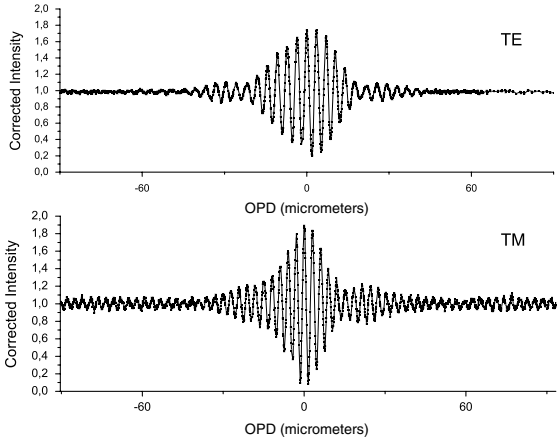

Fig. 1. Polychromatic fringe packets obtained in TE and TM modes with a 12-m-wide Y junction. The TE contrast obtained (79%) is lower than the TM one (91%) because the TE guidance is not as single mode as the TM one.

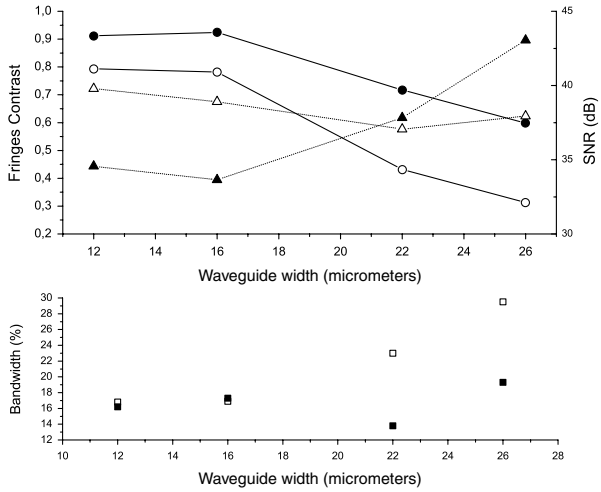

Fig. 2. Top: contrast of fringes and SNR relative to waveguide width. Circles and solid curves correspond to contrast, and triangles and dotted curves to SNR. Bottom: bandwidth relative to waveguide width (in both cases; TE, open symbols; TM, solid symbols).

As Fig. 2 shows, the best contrast (91.2%) is achieved in TM mode with a 12-μm-wide waveguide and a bandwidth of 16.2%. We observe that the contrast decreases, whereas the spectral bandwidth improves as the width increases and the waveguides are more and more multimode. This study allows us to choose $w = 14$ μm as the optimal Y junction, on which we are going to lay the modulating electrodes.

Active junctions. First, we used a moving mirror as an external modulation to scan monochromatic fringes in the electrode-coated device. The monochromatic fringes measured in this way, for both polarizations, are given in Fig. 3. The best rejection ratio obtained is around 2000, for TE polarization. As TM fringes are too close to the noise level, even below for some, it would not be relevant to measure their rejection ratio.

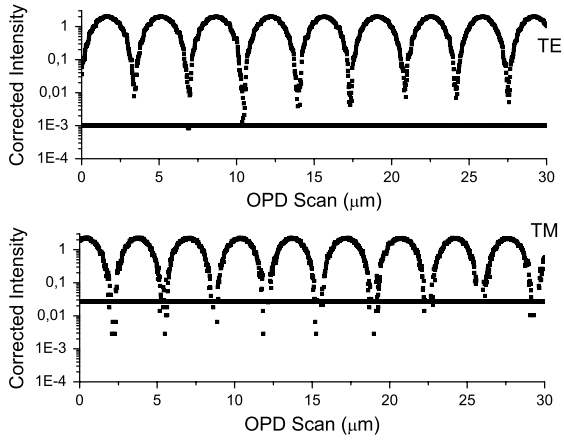

Fig. 3. Monochromatic fringes obtained by external modulation in TE and TM polarizations. Top: the bottom 10^{-3} line corresponds to the noise level. Bottom: the 0.027 line corresponds to the noise level, which is comparatively higher than in the TE polarization.

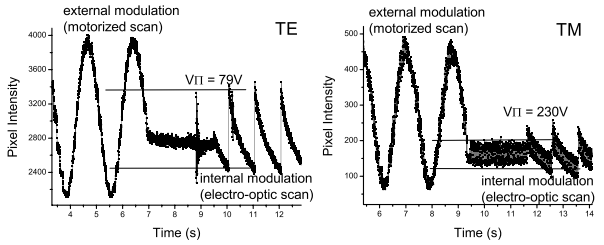

Fig. 4. External modulation and on-chip modulation in the TE (left) and TM (right) modes with monochromatic light.

Both polarizations are guided and recombined but the TM mode is more leaky (especially in the bendings) than the TE one since the birefringence obtained by Ti:diffusion is around 3 times lower for the ordinary index (related to TM in x cut) than for the extraordinary index. Actually, we are working on optimizing this point by changing the way of inducing the index modification in the LN bulk, using ultrafast laser photoinscription [9].

Internal modulation, monochromatic. We finally studied on-chip modification of OPD by applying an electric field in the extraordinary direction of the crystal (z axis, r_{33} of LN). A generator delivered a ramp of 40 Vpp at $f = 1$ Hz on the electrodes. This transverse configuration allows us to modulate the TE and TM modes, respectively, making use of the r_{33} and r_{13} electro-optic coefficients. Figure 4 shows the modulation results in the TE and TM modes.

The V_π voltage is measured by comparison with the external modulation. In our case, as our electrode is 2.6 cm long, the $V_\pi \cdot L_{\text{electrode}}$ is 230 V · 2.6 cm in TM mode and 79 V · 2.6 cm in TE mode. This result is in good agreement with the theory because $V_{\pi\text{TM}} = 2.91 V_{\pi\text{TE}}$, as expected for LN transverse modulators, where r_{33} is 3 times greater than r_{13}. These half-wave voltages are not competitive with other similar studies [5,10], but we are working on their optimization by reducing the silica buffer thickness and the distance between the electrodes. However, this is the first time, to our knowledge, that both TE and TM polarizations are modulated in the same device at this wavelength.

Internal modulation, wide band. On-chip modulation of the fringes, in the wideband regime, was also obtained, showing that it is possible to scan the central maximum, for both polarizations. However, as the V_π is yet too high, we were not able to scan the whole central packet, up to the first coherence length, with this simple function generator.

In conclusion, we have obtained for the first time, to our knowledge, simultaneous TE and TM on-chip modulation in $LiNbO_3$ active Y junctions. High bandwidth and rejection ratios are obtained, confirming the potential of this material for integrated optics applications in the field of stellar interferometry. Future work will address the problem of leakages for TM polarization, as well as optimization of the electro-optical field interaction, by means of new technological developments. We are working on the improvement of the lithographic process in order to increase the overlap between applied electric field and optical mode.

We thank Agence Nationale de la Recherche, ANR-JC09-507107, for funding this project, and P. Kern and J. B. Le Bouquin for useful discussion and technical support.

References

1. R. F. Knacke and W. Kraetschmer, Astron. Astrophys. **92**, 281 (1980).
2. D. Sudarsky, A. Burrows, and I. Hubeny, Astrophys. J. **588**, 1121 (2003).
3. R. Visser, V. Geers, C. Dullemond, J.-C. Augereau, K. Pontoppidan, and E. van Dishoeck, Astron. Astrophys. **466**, 229 (2007).
4. S. Heidmann, O. Caballero, A. Nolot, M. Gineys, T. Moulin, A. Delboulbé, L. Jocou, J.-B. L. Bouquin, J.-P. Berger, and G. Martin, Proc. SPIE **8071**, 807108 (2011).
5. H.-K. Hsiao, K. Winick, J. Monnier, and J.-P. Berger, Opt. Express **17**, 18489 (2009).
6. T. Kawanishi, T. Sakamoto, M. Tsuchiya, and M. Izutsu, in *ECOC 2005. 31st European Conference on Optical Communication, 2005* (2005), Vol. 4, pp. 841–842.
7. N. Grossard, B. Pedron, J. Hauden, and H. Porte, in *JNOG Proceedings*, *ME7* (2007), pp. 110–112.
8. V. C. du Foresto, G. Perrin, and M. Boccas, Astron. Astrophys. **293**, 278 (1995).
9. A. Rodenas, G. Martin, B. Arezki, N. D. Psaila, G. Jose, A. Jha, L. Labadie, P. Kern, A. K. Kar, and R. R. Thomson, Opt. Lett. **37**, 392 (2012).
10. S. Heidmann, A. Delboulbé, T. Moulin, G. Ulliac, N. Courjal, and G. Martin, in *CLEO/Europe and EQEC 2011*, Conference Digest (Optical Society of America, 2011), paper JSIII25.